JOURNAL OF MATERIALS SCIENCE **34** (1999) 4975–4983

An investigation of the hydration chemistry of ternary blends containing cement kiln dust

T. D. DYER, J. E. HALLIDAY, R. K. DHIR
Concrete Technology Unit, University of Dundee, DD1 4HN, UK
E-mail: r.k.dhir@dundee.ac.uk

During the manufacture of Portland cement, dust is generated composed of particles of feedstock and condensed volatilised inorganic salts. Due to its highly alkaline soluble fraction, the dust can be used as an activator in blends containing pozzolanic materials or hydraulic slags, allowing them to undergo cementitious reactions. The inclusion of Portland cement in such blends enhances strength development further, although careful proportioning of materials will be required to obtain optimum performance. Ternary systems containing cement kiln dust, pulverised-fuel ash and Portland cement were characterised in this paper in terms of strength development and hydration products. For a given Portland cement content, optimum strength was achieved in blends containing approximately 10% cement kiln dust for Portland cement levels up to 80%. Beyond this level a CKD/PFA ratio of one was optimal. Isothermal conduction calorimetry results and measurements of calcium hydroxide levels indicated that this was due to an acceleration of the reactions of the blend constituents by the dust. Additionally, the chemical composition of the optimal blends promoted the production of calcium aluminate and ferrite hydrates of a type conducive to maintaining the integrity of the cementitious matrix.

1. Introduction

The manufacture of Portland cement involves the calcining and sintering of feedstock materials in a rotating, cylindrical kiln. The process generates exhaust gases which carry with them dust particles and volatilised inorganic substances. The volatile compounds condense on the dust particles as the gases are cooled and the resulting cement kiln dust (CKD) is collected using electrostatic precipitators. It is estimated that approximately 30 million tonnes of CKD is generated worldwide per year, and whilst some of the dust can be returned to the kiln as part of the feedstock, problems can be encountered if this is permitted to an excessive extent. As a result, there are vast quantities of CKD stockpiled. Since such stockpiling is no longer considered to be a sustainable practice, applications for the use of CKD are being sought.

2. Exploiting CKD properties in cementitious blends

The composition and mineralogy of CKD is dependent on the raw materials used, the type of kiln, and individual plant practices. However, commonly encountered compounds include alkali chlorides and sulfates, as well as calcite and lime. A significant proportion of the dust is soluble in water and the resulting solutions are highly alkaline. The use of alkaline waste materials as activators for pozzolanas and hydraulic slags to create binders is an established practice in the construction industry, and the suitability of using calcined CKD as such a material has previously been demonstrated [1]. However, such formulations generally react slowly, and only limited compressive strength is achieved. The inclusion of Portland cement (PC) in the blend offers the opportunity of obtaining a wider range of strengths via the PC's own cementitious reactions and the generation of portlandite (calcium hydroxide) which takes part in pozzolanic reactions. However, careful formulation of such blends is required to ensure optimum properties are achieved for a given PC content. This paper reports on some of the findings of a study aimed at characterising such ternary blends in terms of strength development and relating this to the reaction products formed.

Two CKDs (identified as A and B) were used for the study, with a pulverised-fuel ash (PFA) as the pozzolanic constituent. The chemical compositions of these materials, as well as the PC used, are given in Table I. Table II shows the estimated proportions of compounds present in the CKD's, identified using X-ray diffraction. Estimation of the quantities of each compound present was carried out by Rietveld refinement on X-ray diffraction traces over an angular range of 3 to 80 $^{\circ}2\theta$ using the computer programs KOALARIET and X-FIT [2–7]. Structural data for the refinements were obtained from the Inorganic Chemical Structures Database held by the EPSRC's Chemical Database Service [8].

The CKD/PFA/PC blends investigated are shown in Fig. 1 in the form of a ternary diagram having a single

TABLE I Results of XRF analysis of CKD, PFA and PC samples

	Concentration (% wt)			
	CKD A	CKD B	PC	PFA
SiO_2	34.3	12.2	21.1	54.2
TiO_2	0.0	0.1	0.2	1.0
Al_2O_3	3.5	3.2	5.0	27.4
Fe_2O_3	2.0	1.8	2.7	6.4
MnO	0.0	0.0	0.1	0.1
MgO	0.8	0.9	1.6	2.1
CaO	34.3	34.8	64.9	4.3
Na_2O	1.2	1.6	0.3	1.4
K_2O	8.2	7.5	0.6	1.7
P_2O_5	0.10	0.1	0.08	0.2
SO_3	11.4	10.6	3.3	0.4
Cl	8.1	2.8	0.03	0.01

TABLE II Estimated quantities of compounds present in CKD samples identified using XRD

	Estimated proportion present (% wt)	
Compound	CKD A	CKD B
$CaCO_3$ (calcite)	8.9	52.8
CaO (lime)	—	1.4
$Ca(OH)_2$ (portlandite)	26.5	8.4
$CaSO_4$ (anhydrite)	9.8	6.1
SiO_2 (quartz)	3.5	6.9
Na_2SO_4 (thenardite)	7.9	—
$Ca_2Al(OH)_6Cl_2(H_2O)_2$ (Friedel's salt)	3.1	—
$Na_{0.31}K_{0.69}Cl$[a] (halite, potassian)	—	2.9
$K_3Na(SO_4)_2$ (aphthitalite)	—	10.2
$K_2Al_4(Si_6Al_2O_{20})(OH)_4$ (muskovite 2m1)	—	3.3
$Ca_2Si_{12}Al_4O_{32}(H_2O)_{12}$[b] (calcium harmotome)	—	0.9
KCl (sylvite)	20.4	7.0
$K_2Ca(SO_4)\cdot H_2O$ (syngenite)	19.9	—

[a]Composition estimated as part of Rietveld refinement.
[b]Barium harmotome structure was used, with barium replaced by calcium.

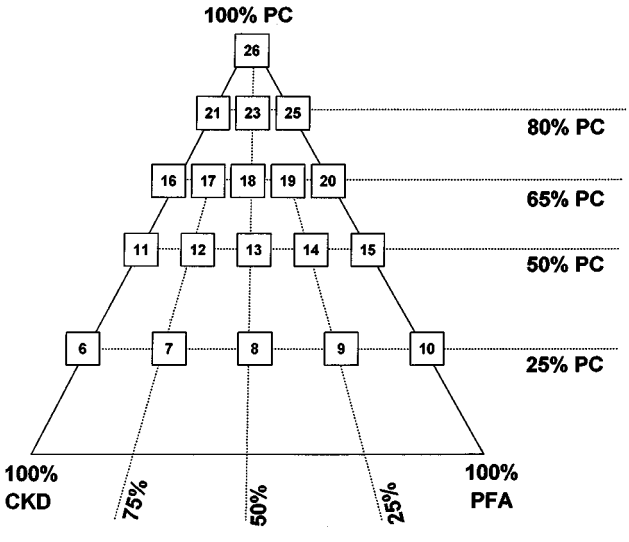

Figure 1 Blends investigated in the ternary CKD-PFA-PC system.

blend constituent at each corner. Numbers 6 to 26 (excluding numbers 22 and 24) are allocated to the blends investigated, and these are used as a means of identification in this paper.

3. Compressive strength development

Mortars containing the blends were mixed in accordance with BS EN 196 part 1 [9] with 450 g of binder blend, 1350 g of sand and 225 g of water. Three 40 × 40 × 160 mm prism moulds were filled in two layers, and each layer compacted using a vibrating table. The tops of the moulds were then covered to prevent evaporation before being transferred to a 95%RH curing room kept at 20 °C. After 24 h the prisms were demoulded and transferred to a water-filled curing tank maintained at 20 °C. Prisms were removed at ages of 2, 7 and 28 days subsequent to mixing and split in half before carrying out compressive strength measurements on the two halves using 40 × 40 mm platens and a loading rate of 2400 Ns^{-1}.

Fig. 2 shows ternary diagrams with contours of equivalent compressive strength at ages of 2, 7 and 28 days for the mortars made with both CKDs A and B. At 2 days, the presence of CKD has the effect of producing strengths which are less than those of PC/PFA blends with the same PC content (those running along the far right-hand edge of the ternary diagram). However, at later ages a region of optimum strength begins to become apparent in blends containing CKD. In the case of both CKD A and B this optimum seems to occur at CKD contents of around 10% up to a PC content of around 80%, above which the optimum would appear to exist at CKD to PFA ratios of 1 : 1. It should be noted that in the case of CKD B the strength of blend 9 drops significantly between 7 and 28 days. This was attributed to cracking observed in this mortar and also observed in blends 6 to 8.

4. Isothermal conduction calorimetry

The hydration of Portland cement leads to the evolution of heat and, hence, isothermal conduction calorimetry is a useful tool for deducing factors related to reaction kinetics. This technique was therefore used to determine the effects of the kiln dusts on the early hydration characteristics of the blends.

A typical rate of heat evolution plot for PC is shown in Fig. 3. The curve consists of a large initial peak which is predominantly the result of the evolution of heat of wetting and the initial hydrolysis of free lime. This is followed by an induction period during which little heat is evolved, leading to a second peak which corresponds to the renewed hydration of the C_3S and C_3A phases, large-scale growth of hydration products, and, as a result, the setting of the cement and initiation of strength development. Two parameters of this curve can be used to identify and quantify the extent of acceleration or retardation of PC hydration: the maximum rate of heat evolution (Q_{max}) during the second peak, and the time at which this peak occurs (t_{max}) [10]. A relative increase in Q_{max} or a relative decrease in t_{max} generally

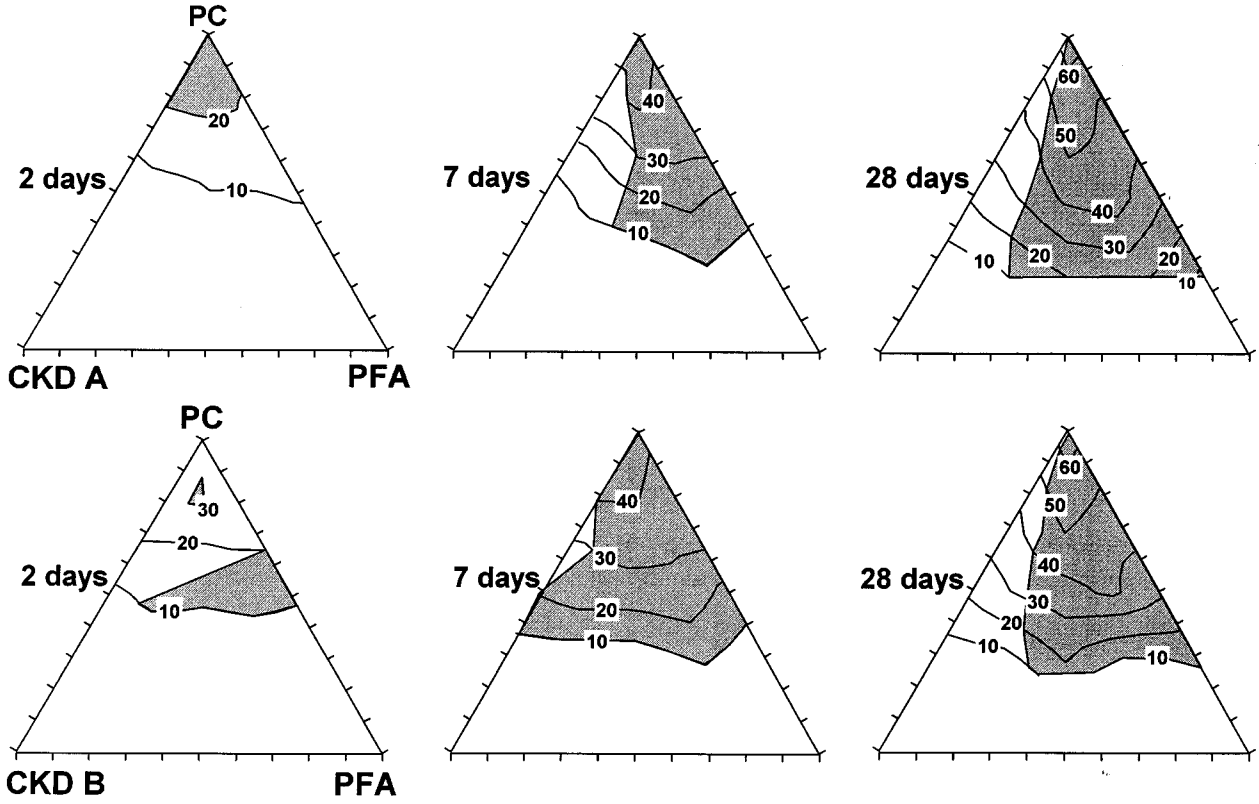

Figure 2 Plots showing compressive strength (N/mm^2) development in blends, containing CKD A and B (shaded regions indicate blends of strength equal to or greater than that of the PC/PFA blend of equal PC content).

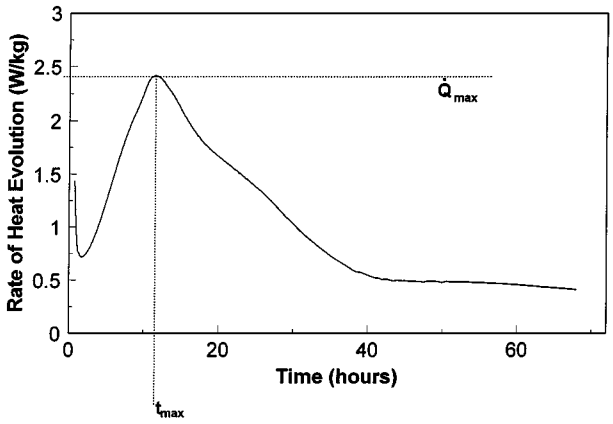

Figure 3 Typical isothermal conduction calorimetry plot obtained from a Portland cement at 17 °C.

indicates acceleration whilst the opposite is observed when cement hydration is retarded.

Isothermal conduction calorimetry was conducted on each blend using 30 g of solids and a water/solids ratio of 0.5. Distilled water was used. The calorimeter was held in a water bath maintained at constant temperature. Whilst the calorimetry experiments were carried out using a bath temperature of 17 °C, compared to a temperature of 20 °C for the other experiments described in this paper, the general trends observed are still valid.

In this instance, mixing of the constituents was carried out prior to the calorimeter's introduction to the water bath. Therefore, the first peak could not be measured accurately, since a short period of time was required to achieve thermal equilibrium.

Figs 4 and 5 show ternary diagrams with contours of equal Q_{max} and t_{max} respectively. The pozzolanic reaction of pulverised-fuel ash begins several days subsequent to mixing and is generally not observed using isothermal conduction calorimetry [11]. Furthermore, whilst it is likely that heat will be evolved from the hydration of CKD compounds, this will be observed during the first peak only. Therefore, the Q_{max} and t_{max} values presented here can be assumed to be exclusively related to PC hydration.

The Q_{max} results suggest that both types of CKD have the effect of accelerating PC hydration. For a given PC content the optimum CKD content with respect to Q_{max} is approximately the same as that observed for strength. It is likely that one of the reasons for the enhancement of compressive strength by CKD, at least at relatively early ages, is its acceleratory effect on PC hydration. However, contrary to the Q_{max} values, the t_{max} values imply that CKD has the effect of retarding hydration. The reason for these conflicting results is uncertain, although it is possible that the combination of potassium chloride, which accelerates hydration [12], and sulfate compounds, which generally accelerate the hydration of calcium silicate cement phases whilst retarding the hydration of calcium aluminate cement phases [13], could produce this effect. It is also possible that the effect could be due to the large quantities of ions released into solution by CKD when mixed with water. This is likely to lead to the formation of a denser membrane of initial hydration products on cement grains. This membrane is believed to limit the movement of ions to and from the unhydrated cement surfaces, thus leading to the induction period [14]. However, the high

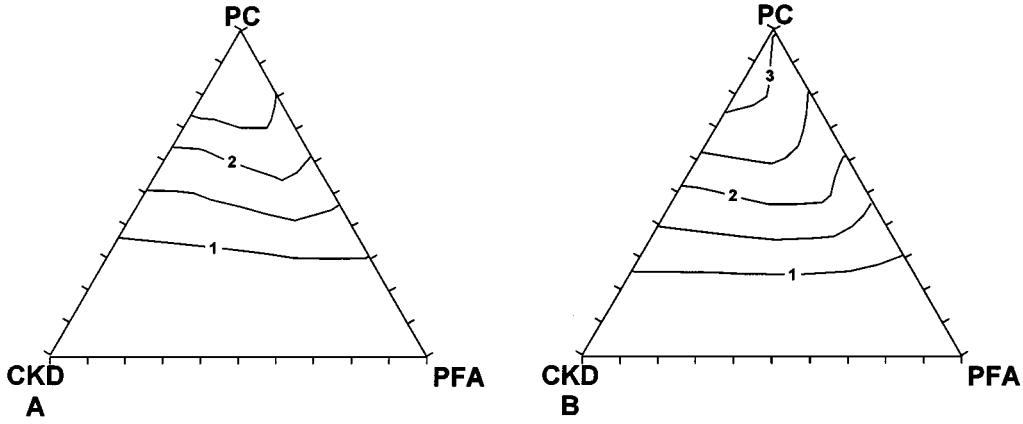

Figure 4 Plots showing Q_{max}(W/kg) measured using isothermal conduction calorimetry for blends containing CKD A and B.

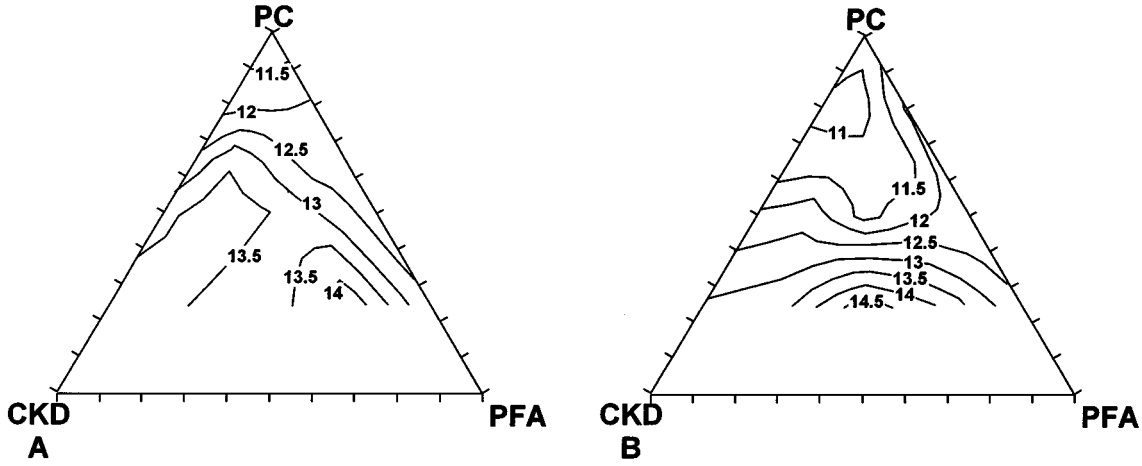

Figure 5 Plots showing t_{max} (hours) measured using isothermal conduction calorimetry for blends containing CKD A and B.

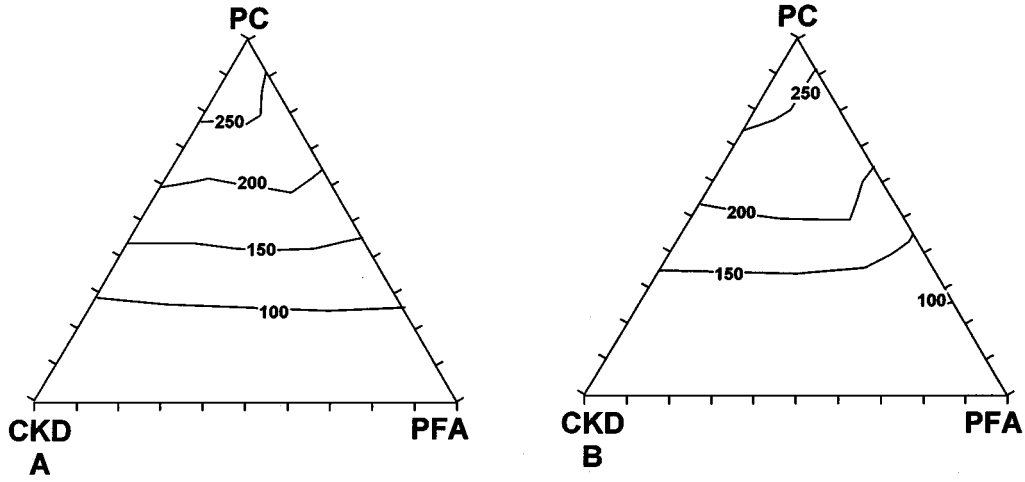

Figure 6 Total heat evolved after 72 h hydration (kJ/kg) measured using isothermal conduction calorimetry for blends containing CKD A and B.

pH levels also produced by the dissolution of CKD component compounds is likely to promote the formation of hydration products, thus leading to high T_{max} values.

The total heat evolved after 72 h is shown in Fig. 6. Similar trends to those observed with t_{max} values are visible, although less pronounced—presumably due to the decreased acceleratory effect at later ages.

5. Hydration products

Pastes of each blend with a water/solids ratio of 0.5 were mixed by hand and transferred to cylindrical polyethylene containers (depth 30 mm, diameter 20 mm). These containers were sealed and kept at 20 °C for 24 h to set before being re-opened and transferred to a water-filled curing tank kept at 20 °C. Hardened paste specimens were removed at ages of 2, 7 and 28 days. Hydration

was arrested by grinding each specimen with acetone, and leaving the resulting power in the solvent for 15 min before being dried under vacuum at 40 °C for 6 h. The powdered specimens were then stored in moisture and CO_2 free conditions until analysis. X-ray diffraction (XRD) was carried out on powder samples with a Philips diffractometer using Cuk_α radiation. Simultaneous thermogravimetry and differential thermal analysis (TG/DTA) were also conducted on the powders up to 1000 °C in a nitrogen atmosphere. The hydration products identified using these techniques are discussed below.

5.1. AFt and AFm Phases

During the hydration of PC, the tricalcium aluminate and calcium aluminoferrite phases react in the presence of calcium and sulfate ions (originating from the gypsum which is added in small quantities to cement) to produce ettringite ($3CaO{\cdot}Al_2O_3{\cdot}3CaSO_4{\cdot}31H_2O$) and iron-substituted ettringite respectively [11]. As well as Fe^{3+}, ettringite can also form solid solutions with other cations producing compounds which are collectively referred to as AFt phases. Such phases are also produced during the pozzolanic reaction of PFA. Using XRD and TG/DTA, an AFt phase was observed in the CKD blends discussed here. The phase is referred to throughout this paper as ettringite, although it is recognised that other ions substituted for aluminium are present.

As PC hydrates, the availability of sulfate ions decreases to a point at which further production of ettringite becomes impossible. At this stage, further hydration of tricalcium aluminate and calcium aluminoferrite leads to the conversion of ettringite to monosulphoaluminate hydrate ($3CaO{\cdot}Al_2O_3{\cdot}CaSO_4{\cdot}12H_2O$) [15]. There are a range of similar compounds which can contain chloride, carbonate and other anions in place of sulfate, although, unlike calcium monosulphoaluminate, ettringite will not take part in their formation and the presence of sufficient sulfate ions to form ettringite will render these compounds unstable [16]. As for ettringite, other cations can also be substituted for Al^{3+}. These compounds are collectively known as AFm phases.

Fig. 7 shows CKD/PFA/PC blend ternary diagrams with contours of equal intensity for the ettringite X-ray diffraction peak occurring at 9.1 °2θ. At 2 days ettringite is present in higher quantities towards the low PC content end of the two ternary systems with the maximum being observed in blends 9 and 14 for CKD A, and in blend 8 for CKD B. By 7 days a clearer trend is apparent with the highest quantities of ettringite present at 25% PC levels with equal proportions of CKD and PFA. Between 7 and 28 days, whilst there is very little change on the PFA-rich side of the ternary system, quantities of ettringite increase significantly where CKD/PFA ratios are greater than 1. This is the result of the increased quantities of sulfate introduced as part of the CKD, which prevent the conversion of ettringite to AFm phases. Ettringite has a significantly higher volume than the reactants which form it and its production leads to the generation of internal stresses within hydrating binders [17]. The cracks observed in the 25% PC blends containing CKD are almost certainly the result of excessive ettringite formation coupled with low binder matrix strengths.

Two AFm phases were identified in the blends investigated. These were calcium monosulphoaluminate hydrate and calcium monochloroaluminate hydrate ($3CaO{\cdot}Al_2O_3{\cdot}CaCl_2{\cdot}10H_2O$) [18]. The latter

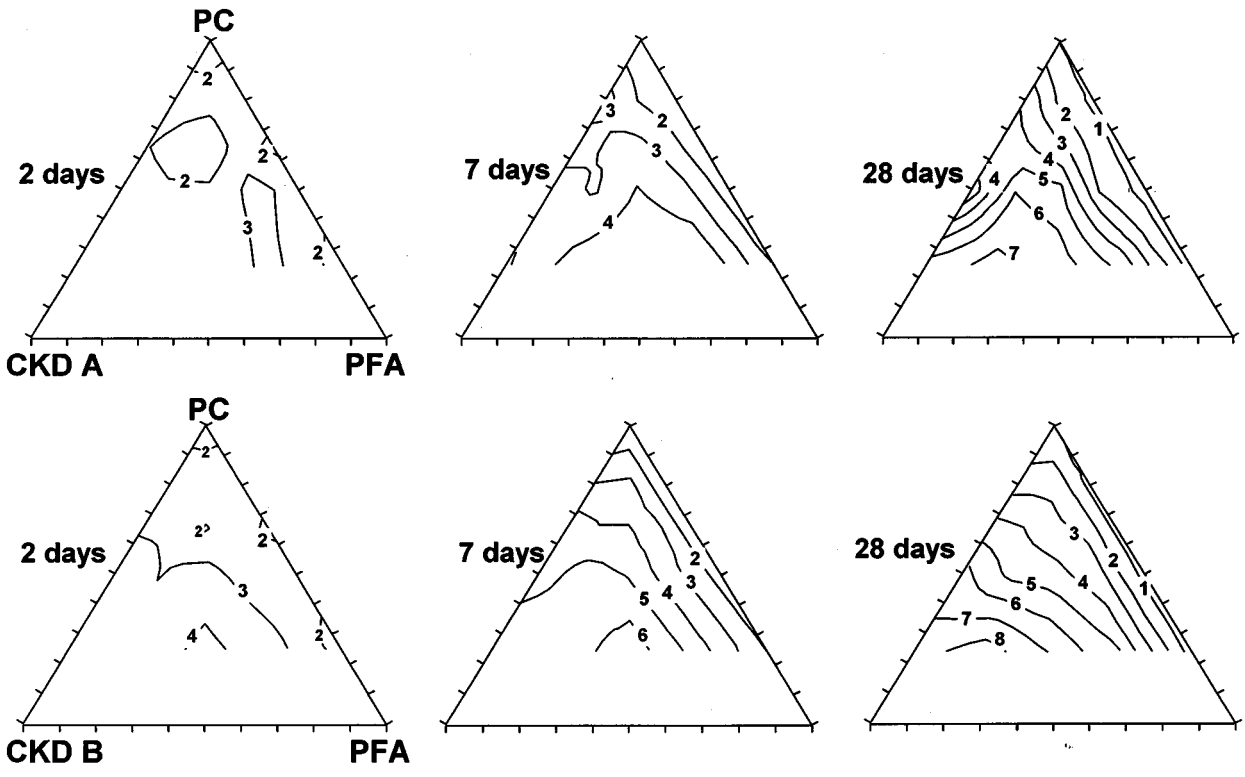

Figure 7 Plots showing XRD peak intensities (expressed as counts $\times 10^{-3}$) for ettringite.

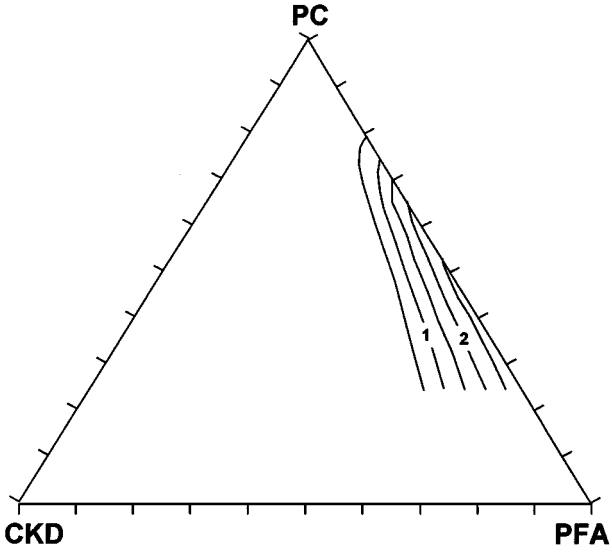

Figure 8 Plot showing XRD peak intensities (expressed as counts $\times 10^{-3}$) for calcium monosulphoaluminate hydrate.

compound is often known as Friedel's salt and is familiar in the fields of concrete durability (where it plays a role in binding chloride ions, thus making a contribution to the protection of steel reinforcement in structures from corrosion [19]), and concrete admixtures (where its formation is observed when $CaCl_2$ is used as an accelerator [20]). Friedel's salt also has an iron analogue ($3CaO{\cdot}Fe_2O_3{\cdot}CaCl_2{\cdot}10H_2O$) [21]. Calcium monosulphoaluminate was only observed in 28 day old blends. Fig. 8 is a ternary diagram showing contours of equal intensity for the calcium monosulphoaluminate X-ray diffraction peak occurring at 9.9 $^\circ 2\theta$. This ternary diagram is the same for both CKDs A and B since the compound was only observed in CKD-free blends. Quantities increase towards the PFA corner of the diagram, which is due to a combination of the high aluminate and low sulphate content of this constituent.

Fig. 9 shows contours of equal intensity for the Friedel's salt X-ray diffraction peak occurring at 11.2 $^\circ 2\theta$ on ternary diagrams for ages of 7 and 28 days. Whilst, in this instance, the formation of Friedel's salt is the result of the high chloride content of CKD, this compound is not present in blends containing larger quantities of CKD, and hence larger quantities of chloride. As mentioned previously, the AFm phases are unstable when sufficient sulfate ions remain for ettringite formation, and, therefore, the regions of the ternary diagrams in which Friedel's salt and calcium monosulphoaluminate are formed are those in which free sulfate ions have been largely consumed.

5.2. Portlandite

Calcium hydroxide ($Ca(OH)_2$) is one of the two main products formed during the hydration of the calcium silicate phases in Portland cement, the other being calcium silicate hydrate (CSH) gel, a substance which makes a significant contribution to strength development. However, due to the inclusion of impurities during its formation in hydrating cement, $Ca(OH)_2$ is usually referred to by its mineralogical title—portlandite. The compound is also sometimes present in CKD, as is the case for CKD A in this study. Portlandite takes part in pozzolanic reactions with certain amorphous siliceous and aluminous materials such as PFA to produce calcium aluminate hydrates and CSH gel. Therefore, by examining changes in portlandite levels, some indication of the extent of pozzolanic reaction can be obtained.

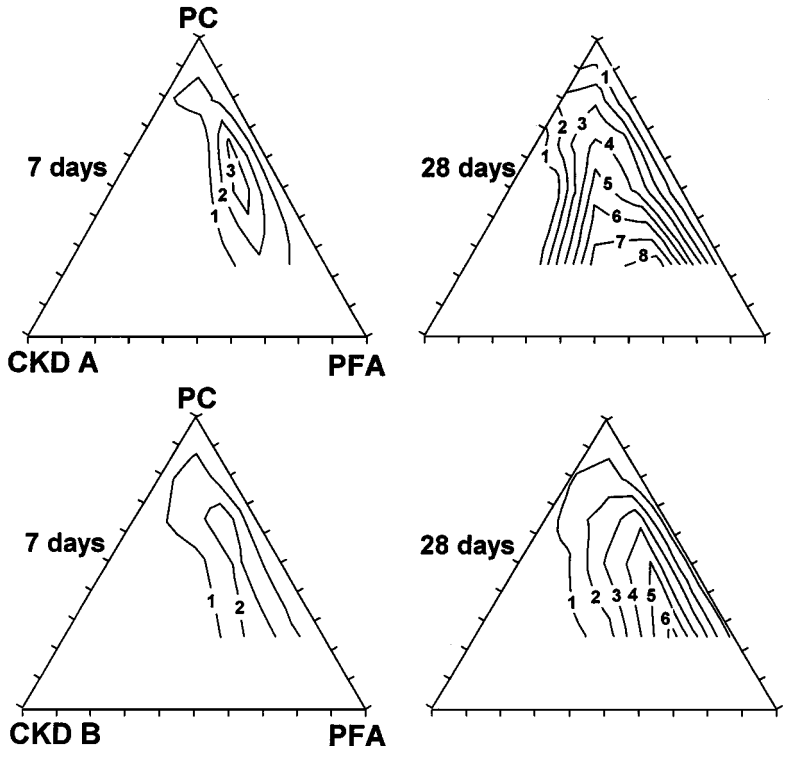

Figure 9 Plots showing XRD peak intensities (expressed as counts $\times 10^{-3}$) for Friedel's salt.

Contoured ternary diagrams for portlandite content are shown in Fig. 10 for CKDs A and B at ages of 2, 7 and 28 days. Quantities were measured using thermogravimetric analysis and are expressed here as a percentage of the residual sample weight at 1000 °C. It should be remembered that CKD A contains significant quantities of portlandite and hence the diagrams for the two different systems are noticeably different. At an age of 2 days both ternary diagrams display features which parallel the acceleratory effects of CKD observed in the Q_{max} isothermal conduction calorimetry results. This is particularly apparent in visual terms in the case of CKD B. As time progresses, portlandite levels begin to decline in certain regions of the ternary systems, particularly in regions with CKD/PFA ratios of less than 1. An estimate of the amount of portlandite that has reacted was made using the equation,

$$C_{\text{reacted}} = C_{\text{tg}} - ((W_{\text{ckd}} \times C_{\text{ckd}}) + (W_{\text{pc}} \times C_{\text{pc}}))$$

where

C_{tg} = weight of portlandite in the sample under investigation, expressed as a percentage of the residual sample weight at 1000 °C,

C_{ckd} = weight of portlandite in the CKD used (if this compound is present) expressed as a per-, centage of the residual CKD sample weight at 1000 °C,

C_{pc} = weight of portlandite in the PC-only blend at the same age as the sample under investigation, expressed as a percentage of the residual PC sample weight at 1000 °C,

W_{ckd} = weight fraction of CKD in the blend under investigation,

W_{pc} = weight fraction of PC in the blend under investigation.

It is stressed that this method does not take into account any acceleration or retardation of PC reactions caused by the presence of CKD and PFA. Therefore, whilst situations in which pozzolanic reactions have occurred to large extents are clearly identified, blends in which the degree of reaction is relatively small may not give a positive result, depending on the influence of the blend constituents on PC hydration kinetics.

A further drawback of the technique becomes apparent when the results for the CKD blends are plotted as ternary diagrams (Fig. 11). In the case of CKD A, it would appear that by an age of 28 days the vast majority of the investigated system has undergone a pozzolanic reaction. This is highly unlikely, since CKD is not a pozzolana. This apparent pozzolanicity is almost certainly the result of the reaction of sulfate compounds other than calcium sulfate (in this case, syngenite) with portlandite to produce ettringite. Such reactions are commonly observed when hydrated cement comes into contact with sulfate solutions, leading to the process known as 'sulfate attack' where the expansive nature of ettringite production in the hardened paste can cause severe damage [22]. Only calcium sulfate was identified in CKD B and, therefore, the non-pozzolanic reaction of portlandite does not occur for this material. Despite the problem of sulfate reactions, it is clear that by 28 days a region on the ternary diagrams for both CKDs begins to become pronounced with respect to portlandite depletion. Again, this region generally coincides with the

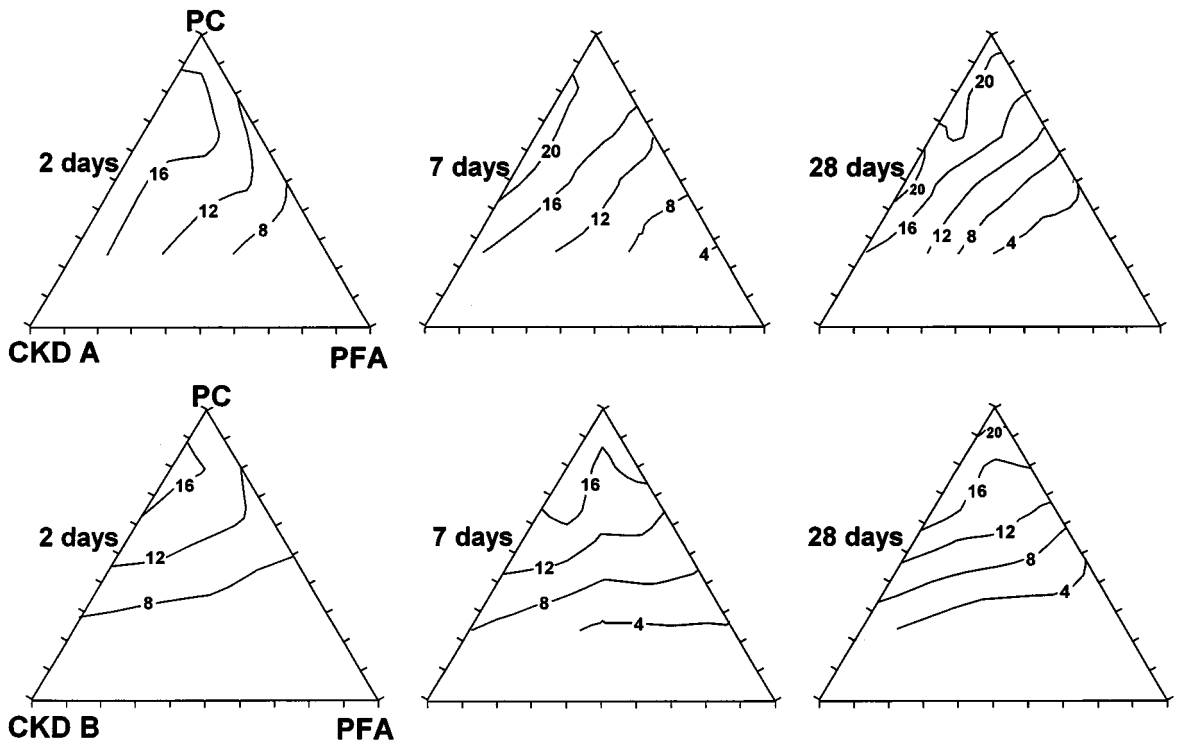

Figure 10 Plots showing portlandite levels in the blends measured using thermogravimetry (expressed as a percentage of the residual sample weight at 1000 °C).

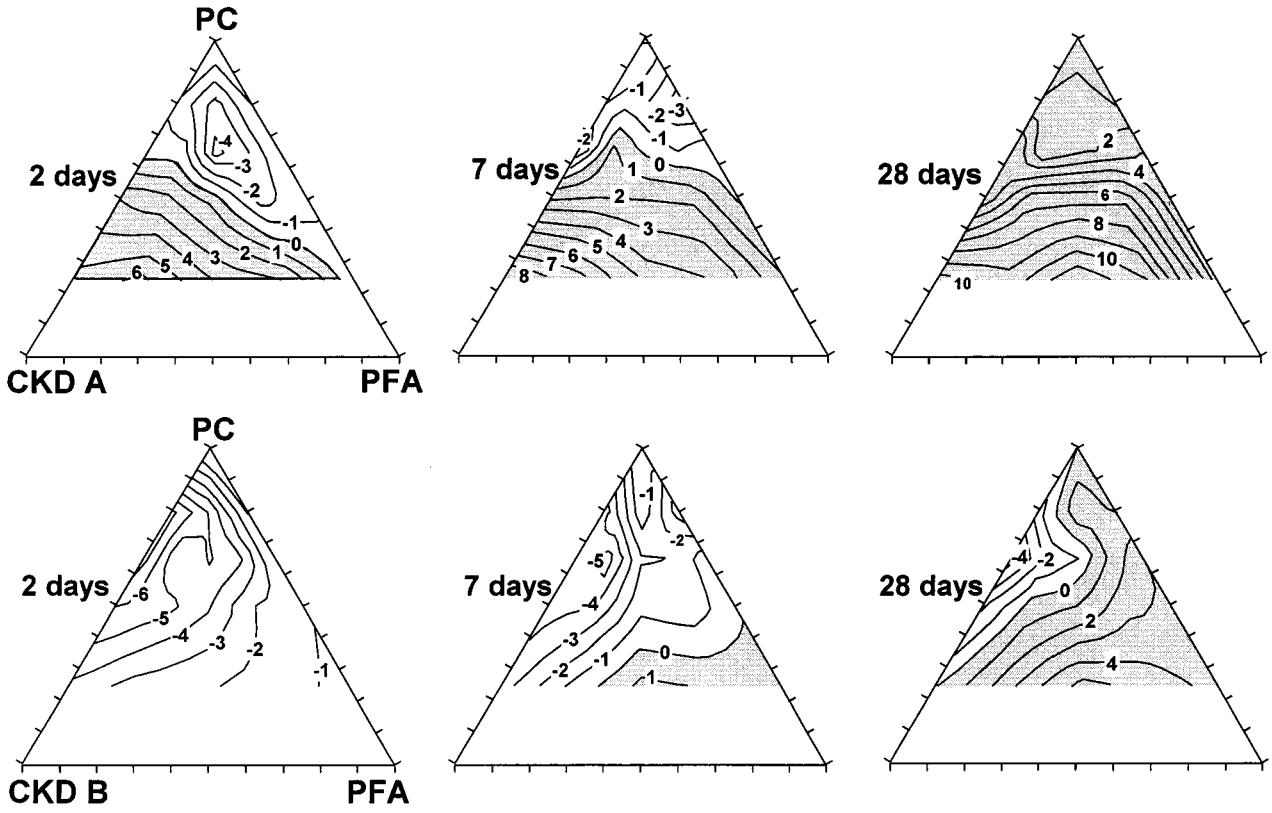

Figure 11 Plots showing estimated quantities of reacted portlandite (expressed as a percentage of the residual sample weight at 1000 °C). Shaded regions indicate blends in which portlandite has reacted.

regions of optimal strength observed previously, and indicates that the higher strengths at certain CKD/PFA ratios would appear to be the result of PFA having reacted to a greater degree.

6. Conclusions

The enhanced strength properties observed in some CKD/PFA/PC blends would appear to be predominantly the result of an increased degree of pozzolanic reaction. This is almost certainly the result of acceleration of the binder reactions by the CKD, as observed using isothermal conduction calorimetry. Whilst this technique only shows the effect on PC reactions, substances which accelerate PC hydration will generally also accelerate PFA reactions.

It should, however, be noted that the regions in which optimal strengths are obtained will also be influenced by the nature of hydration products formed. Most significantly, the halt in the production of ettringite in favour of the less expansive Friedel's salt in regions of optimal strength is likely to also have a beneficial effect in terms of maintaining microstructural integrity.

The presence of chloride salts makes these blends unsuitable for construction involving steel reinforcement, due to the corrosive effect of the chloride ions. Nevertheless, there exists the potential for their use in other applications, for instance, in the manufacture of precast concrete products such as paving slabs. However, a number of issues will first require addressing. Cement kiln dust can contain trace quantities of heavy metals, whose maintained immobilisation within the binder matrix must be ensured [23]. The leaching of large quantities of alkali salts and other bulk constituents which produce surface staining must be minimised through appropriate blend proportions. Additionally, aspects of the chemical composition of cement kiln dust may induce reactions such as delayed ettringite formation and alkali-silica reaction [24, 25] which could have a detrimental effect on the long-term durability of products made from these blends, although suitable materials proportioning may allow such problems to be avoided.

Acknowledgements

The research described in this paper was part of a feasibility study made possible by funding from the EPSRC under its WMR3 programme. The authors are grateful to Mr Paul Livesey, Technical Manager, Castle Cement Ltd, for his advice and assistance with the research programme. We wish to acknowledge the use of the EPSRC's Chemical Database Service at Daresbury.

References

1. A. M. AMIN, EEBIED and H. ELDIDAMONY, *Silicates Industriel* **60** (1995) 109–115.
2. H. BERGER, *X-ray Spectrometry* **15** (1986) 241–243.
3. R. W. CHEARY and A. A. COELHO, *Journal of Applied Crystallography* **25** (1992) 109–121.
4. *Idem., ibid.* **27** (1994) 673–681.
5. *Idem.*, Theoretical model for axial divergence with primary and secondary Soller slits in x-ray line-profile analysis, 1996, in preparation.
6. D. W. MARQUARDT, *Journal of the Society for Industrial and Applied Mathematics* **11** (1963) 431–331.
7. J. C. NASH, "Compact Numerical Methods for Computers" (Adam Hilger, Bristol and New York, 1990).

8. D. A. FLETCHER, R. F. MCMEEKING and D. J. PARKIN, *Journal of Chemical Information and Computer Sciences* **36** (1996) 746–749.
9. British Standards Institution, BS EN 196-1, Methods of testing cement. Part 1: Determination of strength, 1995.
10. D. D. DOUBLE, *Phil. Trans. R. Soc. Lond.* **A310** (1983) 53–66.
11. H. F. W. TAYLOR, "Cement Chemistry" (Academic Press, London,) p. 301.
12. C. R. WILDING, C. R. WALTER and D. D. DOUBLE, *Cement and Concrete Research* **14** (1984) 185–194.
13. S. M. KHALIL and M. A. WARD, *Magazine of Concrete Research* **32** (1980) 28–38.
14. P. BARNES, "Structure and Performance of Cements" (Applied Science Publishers, London, 1983).
15. C. J. WARREN and E. J. REARDON, *Cement and Concrete Research* **24** (1994) 1515–1524.
16. F. ZHANG, Z. ZHOU and Z. LOU, 7th International Congress on the Chemistry of Cement, Paris, 1980, Vol. 2, pp. 88–93.
17. D. MIN and T. MINGSHU, *Cement and Concrete Research* **24** (1994) 119–126.
18. C. ABATE and B. E. SCHEETZ, *J. Amer. Ceram. Soc.* **78** (1995) 939–944.
19. M. A. SANJUÁN, *J. Mater. Sci.* **32** (1997) 6207–6213.
20. V. S. RAMACHANDRAN, "Calcium Chloride in Concrete" (Applied Science, London, 1976) p. 107.
21. A. K. SURYAVANSHI, J. D. SCANTLEBURY and S. B. LYON, *Cement and Concrete Research* **25** (1995) 581–592.
22. P. K. MEHTA, *Cement and Concerete Research* **13** (1983) 401–406.
23. Q. GUO, *Journal of Hazardous Materials* **56** (1997) 181–213.
24. Y. FU and J. J. BEAUDOIN, *J. Mater. Sci. Lett.* **14** (1995) 217–219.
25. J. E. GILLOTT and C. A. ROGERS, *Magazine of Concrete Research* **46** (1994) 99–112.

Received 11 November 1998
and accepted 7 April 1999